



**HAL**  
open science

## Heterobimetallic Ba/Li and Ca/Li amides and diphenylmethanide

Erwann Le Coz, Hanieh Roueindeji, Vincent Dorcet, Thierry Roisnel,  
Jean-François Carpentier, Yann Sarazin

► **To cite this version:**

Erwann Le Coz, Hanieh Roueindeji, Vincent Dorcet, Thierry Roisnel, Jean-François Carpentier, et al.. Heterobimetallic Ba/Li and Ca/Li amides and diphenylmethanide. Dalton Transactions, 2019, 48 (17), pp.5500-5504. 10.1039/c9dt00771g . hal-02120741

**HAL Id: hal-02120741**

**<https://univ-rennes.hal.science/hal-02120741>**

Submitted on 5 Jul 2019

**HAL** is a multi-disciplinary open access archive for the deposit and dissemination of scientific research documents, whether they are published or not. The documents may come from teaching and research institutions in France or abroad, or from public or private research centers.

L'archive ouverte pluridisciplinaire **HAL**, est destinée au dépôt et à la diffusion de documents scientifiques de niveau recherche, publiés ou non, émanant des établissements d'enseignement et de recherche français ou étrangers, des laboratoires publics ou privés.

## Heterobimetallic Ba/Li and Ca/Li amides and diphenylmethanide†

Erwann le Coz,<sup>‡</sup> Hanieh Roueindeji,<sup>‡</sup> Vincent Dorcet, Thierry Roisnel, Jean-François Carpentier and Yann Sarazin\*

The structures of the heterobimetallic Ca/Li and Ba/Li amides  $[\text{CaLi}_2\{\mu^2\text{-N}(\text{SiMe}_2\text{H})_2\}_4]_\infty$  and  $[\text{Ba}_2\text{Li}_2\{\mu^2\text{-N}(\text{SiMe}_2\text{H})_2\}_6]_\infty$ , stabilised by metal...H-Si interactions, and that of a diphenylmethanide calcium salt,  $[\text{Li}(\text{tmeda})_2]^+\cdot[\text{Ca}(\text{CHPh}_2)_3(\text{thf})^-]$ , are presented. These well-defined, storable compounds are inert towards  $\text{Et}_2\text{O}$  and thf.

Heterobimetallic *s*-block complexes often exhibit a positive synergy that renders them more reactive than their individual homometallic components, as epitomised by heterobimetallic bases that enable deprotonation/metalation of weak acids and dehalogenative functionalisation of aromatic substrates. Key reagents include the Lochmann-Schlosser bases  $n\text{BuLi}\cdot\text{KOR}$ ,  $[\text{M}^{(I)}\text{NR}_2\cdot\text{KO}^t\text{Bu}]_n$  superbases for  $\text{M}^{(I)} = \text{Li}$  or  $\text{Na}$ , turbo-Grignards  $\text{RMgX}\cdot\text{LiX}$  where R is an alkyl/aryl group and X is a halide, turbo-Hauser amides  $\text{R}_2\text{NMgX}\cdot\text{LiX}$ ,  $[\text{M}^{(I)}\text{M}'^{(I)}(\text{NR}_2)_2]_n$  where  $\text{M}^{(I)}$  and  $\text{M}'^{(I)}$  are different alkali, and inverse crown ethers  $[\text{M}^{(II)}\text{M}^{(II)}(\text{NR}_2)_2]_{n^{n+}}$  for  $\text{M}^{(II)} = \text{Zn}$  or  $\text{Mg}$ .<sup>1</sup> In view of the diversity of heterobimetallic alkali/Zn and alkali/Mg amides, and despite the current interest in the chemistry of the large alkaline earths calcium, strontium and barium (= Ae),<sup>2</sup> combinations of an alkali metal with Ca, Sr or Ba remain punctual rarities.<sup>3</sup> Two thf solvates,  $[\text{Ca}\{\mu^2\text{-N}(\text{SiMe}_3)_2\}_2\{\text{N}(\text{SiMe}_3)_2\}\text{Li}(\text{thf})]$  (Fig. 1, A) and  $[\text{Ba}\{\text{N}(\text{SiMe}_3)_2\}_2(\text{thf})_3][\text{Li}_2\{\text{N}(\text{SiMe}_3)_2\}_2(\text{thf})_2]$  (B), were reported in 2000.<sup>4</sup> The solvent-free  $[\text{Li}\{\mu^2\text{-N}(\text{SiMe}_3)_2\}_2\text{Ca}\{\text{N}(\text{SiMe}_3)_2\}]$  (C) features  $\text{Ca}\cdots\text{H}_3\text{C}$  and  $\text{Li}\cdots\text{H}_3\text{C}$  agostic interactions.<sup>5</sup>  $[\text{Ca}\{\mu^2\text{-N}(\text{SiMe}_3)_2\}_2\{\text{N}(\text{SiMe}_3)_2\}\text{K}(\text{thf})]$  (D), with its K-coordinated thf and  $\text{K}\cdots\text{H}_3\text{C}$  and  $\text{Ca}\cdots\text{H}_3\text{C}$  agostic contacts, resembles both A and C.<sup>6</sup> Westerhausen described  $[\{(\text{thf})_2\text{K}(\mu^2\text{-NPh}^i\text{Pr})_2\}_2\text{Ca}]$  (E) and showed that  $[\text{K}_2\text{Ca}\{\text{N}(\text{Ph})\text{Me}\}_4]_\infty$  forms a 3-dimensional network while  $[\text{K}_2\text{Ca}(\text{NPh}_2)_4(\text{thf})_3]_\infty$  is linear.<sup>7</sup> Other heterobimetallic Ae/alkali compounds includes alkoxides and aryloxides.<sup>8</sup> Finally, due to the high basicity of alkyl species leading to deprotonation

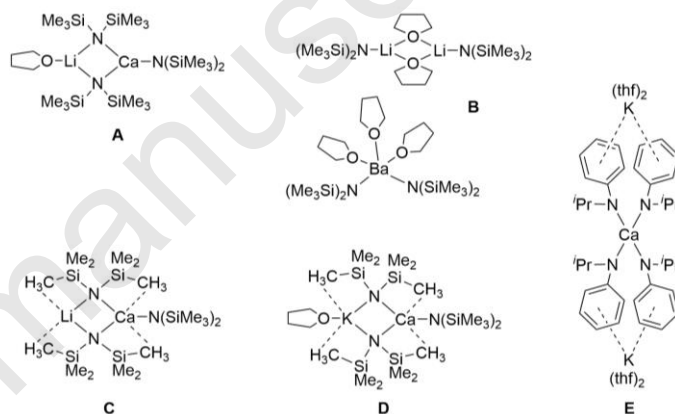


Fig. 1 Known heterobimetallic alkali/Ae amides (Ae = Ca, Sr or Ba).

of even poorly acidic solvents such as ethers, a unique case of structurally characterised heterobimetallic Ae/alkali alkyl compound,  $[\text{Ca}\{\{\mu^2\text{-CH}_2\text{Ph}\}_2\text{Li}(\text{tmeda})\}_2]$ , is known.<sup>9</sup> Of related interest, the calciate and bariate complexes of composition  $[\text{K}^+\cdot\text{Ca}\{\text{CH}(\text{SiMe}_3)_3\}^-]_\infty$  and  $[\text{PBu}_4^+\cdot\text{Cp}_3\text{Ba}^-]_\infty$  have also been described.<sup>10</sup>

The amide  $\text{N}(\text{SiMe}_2\text{H})_2^-$  is nowadays regularly used with alkaline earths to prevent ligand scrambling thanks to stabilising intramolecular  $\text{Ae}\cdots\text{H-Si}$   $\beta$ -agostic interactions.<sup>11</sup> A number of lithium<sup>12</sup> and potassium<sup>13</sup>  $[\text{M}^{(I)}\text{N}(\text{SiR}_2\text{H})_2]_n$  amides exist, for R = Me,  $^i\text{Pr}$ ,  $^t\text{Bu}$  or Ph. The solid-state structures of  $[\text{KN}(\text{SiMe}_2\text{H})_2]_\infty$ ,<sup>11a</sup>  $[\text{Ca}\{\mu^2\text{-N}(\text{SiMe}_2\text{H})_2\}\{\text{N}(\text{SiMe}_2\text{H})_2\}(\text{thf})_2]_2$ ,<sup>11h</sup>  $[\text{Sr}_2\{\text{N}(\text{SiMe}_2\text{H})_2\}_4(\text{thf})_3]^{11g}$  and  $[\text{Ba}\{\text{N}(\text{SiMe}_2\text{H})_2\}_2(\text{thf})_4]^{11b}$  have been established by X-ray diffraction, whereas the trinuclear  $[\text{Ca}_3\{\mu^2\text{-N}(\text{SiMe}_2\text{H})_2\}_4\{\text{N}(\text{SiMe}_2\text{H})_2\}_2]$  was characterised by NMR spectroscopy.<sup>11k</sup> These data highlight a size-dependent variety of coordination patterns in the chemistries of alkali and alkaline earth tetramethyldisilazides.

As part of our ongoing studies in the area of alkaline earth chemistry, we report here on the solid-state structures of Ca/Li and Ba/Li heterobimetallic amido species, and we also describe a rare example of alkyl Ca/Li ate complex that is stable in thf.

Univ Rennes, CNRS, ISCR (Institut des Sciences Chimiques de Rennes) – UMR 6226, F-35000 Rennes, France.

E-mail: yann.sarazin@univ-rennes1.fr; Tel: (+33) 2 23 23 30 19.

† Electronic Supplementary Information (ESI) available: all synthetic, structural and analytical details for compounds 1-3 (CCDC 1896015-1896017). See DOI: 10.1039/x0xx00000x

The heterobimetallic compounds  $[\text{CaLi}_2\{\mu^2\text{-N}(\text{SiMe}_2\text{H})_2\}_4]_\infty$  (**1**) and  $[\text{Ba}_2\text{Li}_2\{\mu^2\text{-N}(\text{SiMe}_2\text{H})_2\}_6]_\infty$  (**2**) were isolated by mixing  $[\text{LiN}(\text{SiMe}_2\text{H})_2]_n$  with, respectively,  $[\text{Ca}\{\text{N}(\text{SiMe}_2\text{H})_2\}_2]_3$  (in pentane) or  $[\text{Ba}\{\text{N}(\text{SiMe}_2\text{H})_2\}_2]_\infty$  (in toluene). The formulations for **1** and **2** were established on the basis of their spectroscopic and crystallographic data. Bulk purity was attested by  $^1\text{H}$  and  $^{13}\text{C}$  NMR spectroscopy recorded in  $\text{thf-}d_8$ . Both compounds were isolated in quantitative yields as colourless solids by adjusting the Ca/Li (1:2) and Ba/Li (1:1) ratios of starting materials to the stoichiometry requested in the final products. However, **1** was also obtained cleanly but in 50% yield by reacting equimolar amounts of  $[\text{LiN}(\text{SiMe}_2\text{H})_2]_n$  and  $[\text{Ca}\{\text{N}(\text{SiMe}_2\text{H})_2\}_2(\text{thf})]$ . Both complexes, and especially **2**, display limited solubility in alkanes and even in aromatic hydrocarbons and, most importantly, they are soluble and do not show signs of decomposition in ethers (e.g. the formation of enolates due to  $\alpha$ - or  $\beta$ -deprotonation of the solvent was not detected).

Single crystals of **1** suitable for XRD analysis were grown from a saturated pentane solution stored at  $-30^\circ\text{C}$ . The complex forms an infinite one-dimensional coordination polymer in the solid state owing to the presence of intermolecular  $\text{Li}\cdots\text{H-Si}$  agostic interactions (Fig. 2). The metallic core made of one  $\text{Ca}^{2+}$  and two  $\text{Li}^+$  metal ions at the centre of

the repetitive unit is held together by four  $\mu^2$ -bridging amido groups. In addition,  $\text{Ca}^{2+}$  ions exhibit four  $\text{Ca}\cdots\text{H-Si}$  agostic contacts with neighbouring H atoms, with  $\text{Ca}(1)\text{-H}(1)$  and  $\text{Ca}(1)\text{-H}(11)$  interatomic distances of, respectively, 2.624(19) and 2.918(18) Å. These values are in the range expected for  $\text{Ca}\cdots\text{H-Si}$  secondary interactions.<sup>11</sup> Note that  $\text{SiH}$  hydrogen atoms were introduced in the structural model through Fourier difference maps analysis. These  $\text{Ca}\cdots\text{H-Si}$  contacts induce severe structural distortions in the  $\text{N}(\text{SiMe}_2\text{H})_2^-$  fragment, best illustrated by the large differences in the pertaining Ca-N-Si angles. Hence,  $\text{Ca}(1)\text{-N}(11)\text{-Si}(11)$  ( $104.66(6)^\circ$ ) is much more acute than its counterpart  $\text{Ca}(1)\text{-N}(11)\text{-Si}(12)$  ( $120.56(7)^\circ$ ) not involved in  $\beta$ -agostic contacts. The distortion is greater in the amide corresponding to  $\text{N}(1)$  ( $\text{Ca}(1)\text{-N}(1)\text{-Si}(1) = 98.04(6)^\circ$ ;  $\text{Ca}(1)\text{-N}(1)\text{-Si}(2) = 125.53(7)^\circ$ ), but direct comparison of the two Ca-N-Si angles in this fragment is thwarted by the additional presence of intermolecular contacts  $\text{Si}(2)\text{-H}(2)\cdots\text{Li}(1^{\text{ii}})$ . The  $\text{Li}(1^{\text{ii}})\text{-H}(2)$  interatomic distance of 2.011(20) Å is much shorter than for  $\text{Ca}\cdots\text{H-Si}$  contacts, in line with the smaller ionic radius of the ion  $\text{Li}^+$  (0.59 Å for C.N. = 4) compared to that of  $\text{Ca}^{2+}$  (1.00 Å for C.N. = 6); it is however longer than in gem-dilithiosilane  $[(\text{R}_2\text{SiLi}_2)(\text{R}_2\text{HSiLi}_2)]$  (1.900(5) Å) and in the dimerised hydridosilyllithium  $[(\text{R}_2\text{HSiLi})_2]$  (1.840(5) and 1.960(5) Å), where  $\text{R} = \text{SiMe}^t\text{Bu}_2$ .<sup>14</sup> As a result of  $\text{Li}\cdots\text{H-Si}$  interactions, the geometry about lithium is trigonal planar ( $\Sigma\theta\text{Li}(1) = 359.15^\circ$ ).

The spectroscopic data for crystals of polymer **1** confirm the presence of metal $\cdots\text{H-Si}$  interactions, although it was not possible to discriminate the two main types of interactions, with lithium and calcium. The solid-state FTIR spectrum of the complex exhibits two peaks corresponding to the stretching of the Si-H bonds: a very large, intense peak with a maximal absorbance at  $1944\text{ cm}^{-1}$ , and another one at  $2035\text{ cm}^{-1}$ . These values, especially that at lowest wavenumber, attest to the existence of multiple  $\text{Ca}\cdots\text{H-Si}$  interactions in the solid-state. By comparison, non-interacting Si-H moieties in metal complexes typically give  $\nu(\text{Si-H})$  located at  $2070\text{ cm}^{-1}$  or greater wavenumbers, while for the parent amine  $\text{HN}(\text{SiMe}_3)_2$ ,  $\nu(\text{Si-H})$  is found at  $2122\text{ cm}^{-1}$ . The  $^1\text{H}$  NMR spectrum recorded in benzene- $d_6$  presents the two expected resonances at 4.80 and 0.31 ppm for  $\text{SiH}$  and  $\text{SiCH}_3$  hydrogens. Limited solubility of **1** in benzene and rather broad and ill-defined resonances precluded the determination of the  $^1J_{\text{SiH}}$  coupling constant. Instead, the latter is consistent with fast fluxionality in solution or, perhaps more likely, with the magnetic inequivalence of  $\text{SiMe}_2\text{H}$  moieties in solution. In the  $^7\text{Li}$  NMR spectrum recorded at room temperature, a major (ca. 95%) resonance centred on  $\delta_{7\text{Li}} = 0.38$  ppm is detected, and was assigned to  $[\text{CaLi}_2\{\mu^2\text{-N}(\text{SiMe}_2\text{H})_2\}_4]$ . The broadness of this resonance ( $\Delta\nu_{1/2} = 59\text{ Hz}$ ) suggests the existence of dynamic phenomena in solution, but VT NMR recorded in toluene- $d_8$  did not provide further information. A minor resonance centred on  $\delta_{7\text{Li}} = 1.11$  ppm (ca. 5%) is also visible in the  $^7\text{Li}$  spectrum, but we could not assign it to any specific species with certainty; it may be related to the formation of small oligomers or monomeric species in solution, but evidence to support this claim could not be gathered. DOSY NMR experiments performed in benzene- $d_6$  in this aim were not fully conclusive, although diffusion time – molecular weight

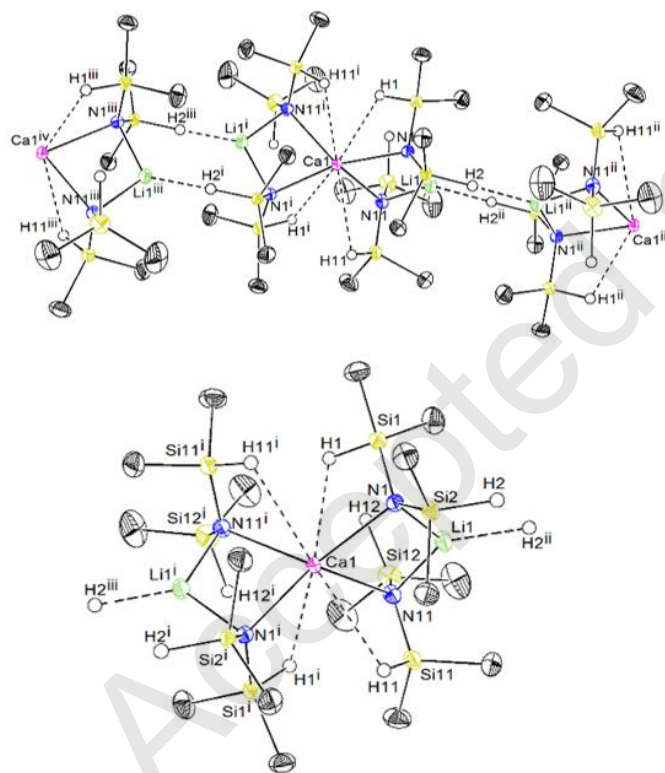
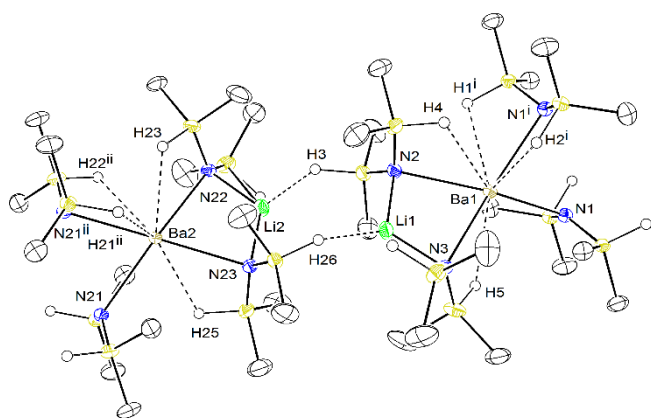


**Fig. 2** ORTEP representation of the solid-state structure of  $[\text{CaLi}_2\{\mu^2\text{-N}(\text{SiMe}_2\text{H})_2\}_4]_\infty$  (**1**), showing the repetitive motif along the 1-D coordination polymer (top) and the details of the coordination sphere around the  $\text{CaLi}_2$  core (bottom). Ellipsoids drawn at the 50% probability level. H atoms other than  $\text{SiH}$  omitted for clarity.  $\text{Ca}\cdots\text{H}$  and  $\text{Li}\cdots\text{H}$  depicted in dotted lines. Colour code: Ca, magenta; Li, green; Si, gold; N, blue; C, black. Selected interatomic distances (Å) and angles ( $^\circ$ ):  $\text{Ca}(1)\text{-N}(1) = 2.5040(13)$ ,  $\text{Ca}(1)\text{-N}(11) = 2.4603(13)$ ,  $\text{Ca}(1)\text{-H}(1) = 2.624(19)$ ,  $\text{Ca}(1)\text{-H}(11) = 2.918(18)$ ,  $\text{Li}(1)\text{-N}(1) = 2.014(3)$ ,  $\text{Li}(1)\text{-N}(11) = 1.994(3)$ ,  $\text{Li}(1)\text{-H}(2^{\text{ii}}) = 2.011(20)$ ;  $\text{N}(1)\text{-Li}(1)\text{-N}(11) = 106.44(13)$ ,  $\text{N}(1)\text{-Li}(1)\text{-H}(2^{\text{ii}}) = 119.31(56)$ ,  $\text{N}(11)\text{-Li}(1)\text{-H}(2^{\text{ii}}) = 133.40(57)$ ,  $\text{Ca}(1)\text{-N}(1)\text{-Si}(1) = 98.04(6)$ ,  $\text{Ca}(1)\text{-N}(1)\text{-Si}(2) = 125.53(7)$ ,  $\text{Ca}(1)\text{-N}(11)\text{-Si}(11) = 104.66(6)$ ,  $\text{Ca}(1)\text{-N}(11)\text{-Si}(12) = 120.56(7)$ .



analysis seems to suggest that **1** exists as isolated  $[\text{CaLi}_2\{\mu^2\text{-N}(\text{SiMe}_2\text{H})_2\}_4]$  in solution in this solvent.<sup>15</sup> The <sup>29</sup>Si NMR spectrum of **1** shows a main and rather broad resonance for all Si atoms centred on  $\delta_{29\text{Si}} = -20.78$  ppm; again, the <sup>1</sup>J<sub>SiH</sub> coupling between Si and H atoms could not be measured. Two additional yet very minor resonances are located at  $\delta_{29\text{Si}} = -17.35$  and  $-24.55$  ppm, also corroborating the possible presence of lower-aggregation species. A single resonance is detected at 4.24 ppm in the <sup>13</sup>C{<sup>1</sup>H} NMR spectrum. On the whole, NMR data did not allow to firmly establish the exact structure of **1** in solution.<sup>15</sup>

**Fig. 3** ORTEP representation of the solid-state structure of  $[\text{Ba}_2\text{Li}_2\{\mu^2\text{-N}(\text{SiMe}_2\text{H})_2\}_6]_\infty$  (**2**). Ellipsoids drawn at the 50% probability level. H atoms other than SiH omitted for clarity. Ba...H and Li...H depicted in dotted lines. Colour code: Ba, brown; Li, green; Si, gold; N, blue; C, black. Representative interatomic distances (Å): Ba1-N1 = 2.774(3), Ba1-N3 = 2.834(3), Ba1-N2 = 2.850(3), Ba1-N1<sup>i</sup> = 2.892(3), Ba1-H1<sup>ii</sup> = 3.20(6), Ba1-H2<sup>ii</sup> = 2.88(5), Ba1-H4 = 2.85(6), Ba1-H5 = 2.99(6), Ba2-N21 = 2.803(3), Ba2-N22 = 2.827(3), Ba2-N21<sup>ii</sup> = 2.839(3), Ba2-N23 = 2.914(3), Ba2-H21<sup>i</sup> = 3.06(5), Ba2-H22<sup>i</sup> = 3.05(6), Ba2-H23 = 2.80(6), Ba2-H25 = 2.89(6), Li1-N2 = 1.993(8), Li1-N3 = 2.001(8), Li2-N22 = 1.999(8), Li2-N23 = 2.014(7), Li1-H26 = 1.98(5), Li2-H3 = 2.00(5).

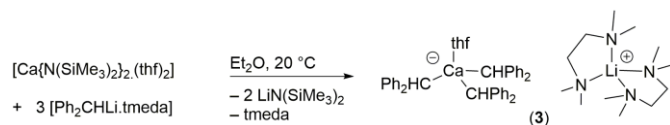
The solid-state structure of complex **2** established by X-ray diffraction crystallography is depicted in Figure 3. Like **1**, due to the existence of Li...H-Si intermolecular interactions, it forms a mono-dimensional coordination polymer made of consecutive enchainment of Ba<sub>2</sub> and Li<sub>2</sub> sequences. Again, SiH hydrogens were localised by Fourier difference maps analysis. The two pairs of barium and lithium ions are crystallographically inequivalent, although the coordination patterns are overall comparable. Each Ba<sup>2+</sup> is coordinated by four nitrogen atoms, with Ba-N bond distances in the range 2.774(3)-2.892(3) Å for Ba1 and 2.803(3)-2.914(3) Å for Ba2. Each also displays four Ba...H-Si contacts, with interatomic distances between 2.88(5)-3.20(6) and 2.80(6)-3.06(5) Å respectively for Ba1 and Ba2. This is similar for instance to the distances measured in the complex  $[\{\text{LO}\}\text{BaN}(\text{SiMe}_2\text{H})_2]$  bearing an aminoether-phenolate ligand  $\{\text{LO}\}^-$  (Ba...H = 2.99(1) Å<sup>11a</sup>) and in  $[\text{Ba}\{\text{N}(\text{SiMe}_2\text{H})_2\}_2\cdot(\text{thf})_4]$  (3.11(2) Å<sup>11b</sup>). Each lithium is coordinated by two N atoms with Li-N distances in the range 1.993(8) to 2.014(7) Å, and is involved in an additional Li...H-Si interaction at 1.98(5) Å for Li1

and 2.00(5) Å for Li2. Related Li...H-Si interactions were longer, at 2.093(2)-2.239(1) Å, in trinuclear  $[\text{LiN}(\text{SiMe}_2\text{tBu})(\text{SiMe}_2\text{H})_3]_3$ .<sup>12d</sup> The NMR data for **2** in benzene-*d*<sub>6</sub> are consistent with the existence of Ba...H-Si interactions. The resonance for the SiH hydrogen is detected at  $\delta_{\text{SiH}} = 4.92$  ppm, and the <sup>1</sup>J<sub>SiH</sub> coupling constant of 160 Hz is consistent with mild Ba...H-Si interactions. This is supported by FTIR analysis, which showed the presence of an intense and broad peak at 1994 cm<sup>-1</sup>, with a smaller shoulder at 1930 cm<sup>-1</sup>.<sup>11a</sup> Complex **2** is to our knowledge the first homoleptic heterobimetallic Ba-alkali amide; distantly related species include  $[\text{Ba}_2\text{Li}\{\text{N}(\text{SiMe}_3)_2\}\{(\text{N}^t\text{Bu})_3\text{S}\}_2\cdot(\text{thf})_2]$ , a thf-supported heteroleptic compound.<sup>16</sup>

The downside of heterobimetallic species **1** and **2** may be their tamed reactivity compared to hexamethyldisilazides. This stems from the lower basicity of the amide  $\text{N}(\text{SiMe}_2\text{H})_2^-$  vs that of  $\text{N}(\text{SiMe}_3)_2^-$  (relative pK<sub>a</sub> in thf 22.6 and 25.8<sup>17</sup>). We hence set out to prepare highly basic diphenylmethanide heterobimetallic species, akin to Ruhlandt-Senge's  $[\text{Ca}\{\{\mu^2\text{-CH}_2\text{Ph}\}_2\text{Li}(\text{tmeda})\}_2]$ .<sup>9</sup> Of note, this compound, of limited solubility in toluene, decomposes immediately in the presence of ethers upon release of enolates.

We found that the reaction of  $[\text{Ca}\{\text{N}(\text{SiMe}_3)_2\}_2\cdot(\text{thf})_2]$  with 3 equivalents of  $[\text{Ph}_2\text{CHLi}\cdot\text{tmeda}]$  in diethyl ether reproducibly affords the salt  $[\text{Li}(\text{tmeda})_2]^+\cdot[\text{Ca}(\text{CHPh}_2)_3(\text{thf})]^-$  (**3**) in ca. 50% yield upon release of  $[\text{LiN}(\text{SiMe}_3)_2]$  (Scheme 1). The composition of **3** was established by XRD-day analysis, after it recrystallised as **3**·Et<sub>2</sub>O with a non-interacting Et<sub>2</sub>O molecule. The formulation was supported by NMR, which also confirmed both sample purity and the presence of thf and tmeda. The compound is very soluble in thf, sparingly so in Et<sub>2</sub>O and insoluble in hydrocarbons. The solid-state structure displayed in Figure 4 shows the actual salt to consist of a discrete separated ion pair

$[\text{Li}(\text{tmeda})_2]^+\cdot[\text{Ca}(\text{CHPh}_2)_3(\text{thf})]^-$  (**3**). Ellipsoids drawn at the 50% probability level. Non-interacting Et<sub>2</sub>O molecule and H atoms omitted for clarity. Only the main component of disordered thf and tmeda molecules are drawn. Colour code: Ca, magenta; Li, green; N, blue; C, black; O, red. Representative interatomic distances (Å) and angles (°): Ca1-O61 = 2.3066(14), Ca1-C7 = 2.575(2), Ca1-C27 = 2.5869(19), Ca1-C47 = 2.612(2), Li1-N4 = 2.086(4), Li1-N3 = 2.115(4), Li1-N1 = 2.121(4), Li1-N2 = 2.129(4); O61-Ca1-C7 = 100.89(6), O61-Ca1-C27 = 106.22(6), C7-Ca1-C27 = 108.76(6), O61-Ca1-C47 = 118.30(6), C7-Ca1-C47 = 106.03(7), C27-Ca1-C47 = 115.39(6), N4-Li1-N3 = 88.65(15), N4-Li1-N1 = 120.65(18), N3-Li1-N1 = 122.17(17), N4-Li1-N2 = 121.43(17), N3-Li1-N2 = 120.46(18), N1-Li1-N2 = 87.30(14).



**Scheme 1.** Synthesis of  $[\text{Li}(\text{tmeda})_2]^+\cdot[\text{Ca}(\text{CHPh}_2)_3(\text{thf})]^-$  (**3**)

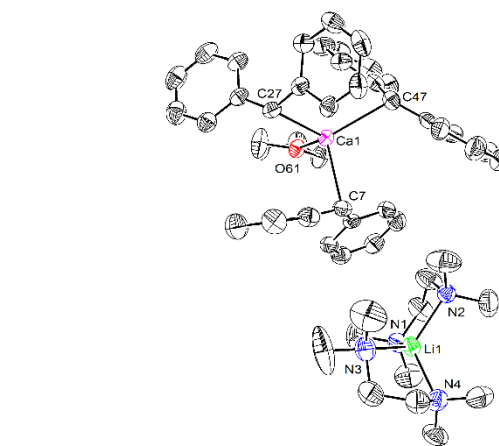


**Fig. 4** ORTEP representation of the solid-state structure of  $[\text{Li}(\text{tmeda})_2]^+\cdot[\text{Ca}(\text{CHPh}_2)_3(\text{thf})]^-$  (**3**). Ellipsoids drawn at the 50% probability level. Non-interacting Et<sub>2</sub>O molecule and H atoms omitted for clarity. Only the main component of disordered thf and tmeda molecules are drawn. Colour code: Ca, magenta; Li, green; N, blue; C, black; O, red. Representative interatomic distances (Å) and angles (°): Ca1-O61 = 2.3066(14), Ca1-C7 = 2.575(2), Ca1-C27 = 2.5869(19), Ca1-C47 = 2.612(2), Li1-N4 = 2.086(4), Li1-N3 = 2.115(4), Li1-N1 = 2.121(4), Li1-N2 = 2.129(4); O61-Ca1-C7 = 100.89(6), O61-Ca1-C27 = 106.22(6), C7-Ca1-C27 = 108.76(6), O61-Ca1-C47 = 118.30(6), C7-Ca1-C47 = 106.03(7), C27-Ca1-C47 = 115.39(6), N4-Li1-N3 = 88.65(15), N4-Li1-N1 = 120.65(18), N3-Li1-N1 = 122.17(17), N4-Li1-N2 = 121.43(17), N3-Li1-N2 = 120.46(18), N1-Li1-N2 = 87.30(14).

made of the  $\text{Ca}(\text{CHPh}_2)_3(\text{thf})^-$  anion and the  $\text{Li}(\text{tmeda})_2^+$  cation. Each metallic ion is four-coordinate, with a distorted tetrahedral environment. The Li-N interatomic distances in the cation (2.086(4)–2.129(4) Å) are unremarkable. The three Ca-C $\alpha$  bond lengths (2.575(2)–2.612(2) Å) in **3** match those in  $[\text{Ca}\{\mu^2\text{-CH}_2\text{Ph}\}_2\text{Li}(\text{tmeda})_2]_n^9$  (2.610(5) Å) and in the monometallic complex  $[\text{Ca}(\text{CH}_2\text{Ph})_2(\text{thf})_4]$  (2.2568(5)–2.595(5) Å).<sup>18</sup> It is worth noting that compound **3** is a well-separated ion pair, whereas  $[\text{Ca}\{\mu^2\text{-CH}_2\text{Ph}\}_2\text{Li}(\text{tmeda})_2]$  is a PhCH<sub>2</sub>-bridged dinuclear complex, and that unlike this complex, **3** is perfectly stable in thf. <sup>1</sup>H and <sup>13</sup>C NMR data for **3** recorded in thf-d<sub>8</sub> demonstrate absence of decomposition in this solvent. The <sup>7</sup>Li NMR spectrum recorded at –60 °C contains a single, sharp resonance at  $\delta_{7\text{Li}} = -0.57$  ppm. In the <sup>1</sup>H NMR spectrum, the Ph<sub>2</sub>CH methanide resonance appears as a singlet at  $\delta_{1\text{H}} = 3.91$  ppm at 25 °C and 4.20 ppm at –60 °C where the spectrum was better resolved and resonances for aromatic hydrogens could be assigned.

In summary, the new amides  $[\text{CaLi}_2\{\mu^2\text{-N}(\text{SiMe}_2\text{H})_2\}_4]_\infty$  (**1**) and  $[\text{Ba}_2\text{Li}_2\{\mu^2\text{-N}(\text{SiMe}_2\text{H})_2\}_6]_\infty$  (**2**), as well as the alkyl salt  $[\text{Li}(\text{tmeda})_2^+\text{Ca}(\text{CHPh}_2)_3(\text{thf})^-]$  (**3**), are readily available. These rare Ae/alkali heterobimetallic complexes are stable, show good solubility properties, and do not decompose in ethers. They may hence be useful as well-defined and storable reagents for stoichiometric functionalisations reactions, and we are currently investigating these alleys.

## Conflicts of interest

There are no conflicts to declare.

## Notes and references

- ‡ These two co-authors have contributed equally to the work.
- For reviews, see: (a) R. E. Mulvey, *Organometallics*, 2006, **25**, 1060; (b) R. E. Mulvey, F. Mongin, M. Uchiyama and Y. Kondo, *Angew. Chem. Int. Ed.*, 2007, **46**, 3802; (c) R. E. Mulvey, *Acc. Chem. Res.*, 2009, **42**, 743; (d) B. Haag, M. Mosrin, H. Ila, V. Malakhov and P. Knochel, *Angew. Chem. Int. Ed.*, 2011, **50**, 9794; (e) A. Harrison-Marchand and F. Mongin, *Chem. Rev.*, 2013, **113**, 7470; (f) F. Mongin and A. Harrison-Marchand, *Chem. Rev.*, 2013, **113**, 7563; (g) D. Tilly, F. Chevallier, F. Mongin and P. C. Gros, *Chem. Rev.*, 2014, **114**, 1207; (h) D. S. Ziegler, B. Wei and P. Knochel, *Chem. Eur. J.*, DOI: 10.1002/chem.201803904.
  - For reviews, see: (a) M. Westerhausen, *Coord. Chem. Rev.*, 2008, **252**, 1516; (b) S. Harder *Chem. Rev.*, 2010, **110**, 3852; (c) M. S. Hill, D. J. Liptrot and C. Weetman, *Chem. Soc. Rev.*, 2016, **45**, 972; (d) M. Westerhausen, A. Koch, H. Görls and S. Kriech, *Chem. Eur. J.*, 2017, **23**, 1456; (e) D. Mukherjee, D. Schuhknecht and J. Okuda, *Angew. Chem. Int. Ed.* 2018, **57**, 9590.
  - M. Westerhausen, *Dalton Trans.*, 2006, 4755.
  - R. P. Davies, *Inorg. Chem. Commun.*, 2000, **3**, 13.
  - A. R. Kennedy, R. E. Mulvey and R. B. Rowlings, *J. Organomet. Chem.*, 2002, **648**, 288.
  - X. He, B. C. Noll, A. Beatty, R. E. Mulvey and K. W. Henderson, *J. Am. Chem. Soc.*, 2004, **126**, 7444.
  - C. Glock, H. Görls and M. Westerhausen, *Inorg. Chem.*, 2009, **48**, 394.
  - (a) P. S. Coan, W. E. Streib and K. G. Caulton, *Inorg. Chem.*, 1991, **30**, 5019; (b) H. Bock, T. Hauck, C. Naether, N. Roesch, M. Stauffer and O. D. Haeberlen, *Angew. Chem., Int. Ed. Engl.*, 1995, **34**, 1353; (c) K. M. Fromm, E. D. Gueneau and H. Goesmann, *Chem. Commun.*, 2000, 2187; (d) P. B. Hitchcock, Q. Huang, M. F. Lappert, X.-H. Wei and M. Zhou, *Dalton Trans.*, 2006, 2991; (e) K. M. Fromm, *Dalton Trans.*, 2006, 5103; (f) W. Maudez, D. Haeussinger and K. M. Fromm, *Z. Anorg. Allg. Chem.*, 2006, **632**, 2295; (g) M. F. Zuniga, G. B. Deacon and K. Ruhlandt-Senge, *Chem. Eur. J.*, 2007, **13**, 1921.
  - M. A. Guino-o, C. F. Campana and K. Ruhlandt-Senge, *Chem. Commun.*, 2008, 1692.
  - (a) P. B. Hitchcock, A. V. Khvostov and M. F. Lappert, *J. Organomet. Chem.*, 2002, **663**, 263; (b) S. Harder, *Angew. Chem. Int. Ed.*, 1998, **37**, 1239.
  - (a) Y. Sarazin, D. Roşca, V. Poirier, T. Roisnel, A. Silvestru, L. Maron and J.-F. Carpentier, *Organometallics*, 2010, **29**, 6569; (b) O. Michel, K. W. Törnroos, C. Maichle-Mössmer and R. Anwander, *Chem. Eur. J.*, 2011, **17**, 4964; (c) O. Michel, S. König, K. W. Törnroos, C. Maichle-Mössmer and R. Anwander, *Chem. Eur. J.*, 2011, **17**, 11857; (d) O. Michel, K. W. Törnroos, C. Maichle-Mössmer and R. Anwander, *Eur. J. Inorg. Chem.*, 2012, 44; (e) B. Liu, T. Roisnel, J.-P. Guégan, J.-F. Carpentier and Y. Sarazin, *Chem. Eur. J.*, 2012, **18**, 6289; (f) B. Liu, T. Roisnel, J.-F. Carpentier and Y. Sarazin, *Angew. Chem. Int. Ed.*, 2012, **51**, 4943; (g) P. Jochmann, J. P. Davin, S. Maslek, T. P. Spaniol, Y. Sarazin, J.-F. Carpentier and J. Okuda, *Dalton Trans.*, 2012, **41**, 9176; (h) J. P. Davin, J.-C. Buffet, T. P. Spaniol and J. Okuda, *Dalton Trans.*, 2012, **41**, 12612; (i) B. Liu, T. Roisnel, J.-F. Carpentier and Y. Sarazin, *Chem. Eur. J.*, 2013, **19**, 2784; (j) B. Liu, T. Roisnel, J.-F. Carpentier and Y. Sarazin, *Chem. Eur. J.*, 2013, **19**, 13445; (k) N. Romero, S.-C. Roşca, Y. Sarazin, J.-F. Carpentier, L. Vendier, S. Mallet-Ladeira, C. Dinoi and M. Etienne, *Chem. Eur. J.*, 2015, **21**, 4115; (l) C. Bellini, V. Dorcet, J.-F. Carpentier, S. Tobisch and Y. Sarazin, *Chem. Eur. J.*, 2016, **22**, 4564; (m) S.-C. Roşca, C. Dinoi, E. Caytan, V. Dorcet, M. Etienne, J.-F. Carpentier and Y. Sarazin, *Chem. Eur. J.*, 2016, **22**, 6505; (n) S.-C. Roşca, E. Caytan, V. Dorcet, T. Roisnel, J.-F. Carpentier and Y. Sarazin, *Organometallics*, 2017, **36**, 1269; (o) D. Mukherjee, S. Shirase, K. Beckerle, T. P. Spaniol, K. Mashima and J. Okuda, *Dalton Trans.*, 2017, **46**, 8451; (p) B. Freitag, J. Pahl, C. Färber and S. Harder, *Organometallics*, 2018, **37**, 469.
  - (a) B. Goldfuss, P. von Ragué Schleyer, S. Handschuh, F. Hampel and W. Bauer, *Organometallics*, 1997, **16**, 5999; (b) K. Junge, E. Popowski, R. Kempe and W. Baumann, *Z. Anorg. Allg. Chem.*, 1998, **624**, 1369; (c) E. Gellermann, U. Klingebiel, T. Pape, F. Dall'Antonia, T. R. Schneider and S. Schmatz, *Z. Anorg. Allg. Chem.*, 2001, **627**, 2581; (e) J. Schneider, E. Popowski and H. Reinke, *Z. Anorg. Allg. Chem.*, 2002, **628**, 719; (d) C. Matthes, M. Noltemeyer, U. Klingebiel and S. Schmatz, *Organometallics*, 2007, **26**, 838.
  - (a) J.-C. Buffet and J. Okuda, *Dalton Trans.*, 2011, **40**, 7748; (b) J. Schneider, E. Popowski and H. Reinke, *Z. Anorg. Allg. Chem.*, 2003, **629**, 55; (c) D. Mukherjee, H. Osseili, T. P. Spaniol and J. Okuda, *Dalton Trans.*, 2017, **46**, 8017.
  - D. Bravo-Zhivotovskii, I. Ruderfer, S. Melamed, M. Botoshansky, B. Tumanskii and Y. Apeloig, *Angew. Chem. Int. Ed.*, 2005, **44**, 739.
  - Compounds **1** and **2** are soluble in thf-d<sub>8</sub>, but their solid-state structures are not maintained in this coordinating solvent. DOSY NMR (diffusion time – molecular weight) analysis of **1** performed in highly dilute benzene-d<sub>6</sub> solution gave an estimated molecular weight (624 g.mol<sup>-1</sup>) close to that expected for an isolated  $[\text{CaLi}_2\{\mu^2\text{-N}(\text{SiMe}_2\text{H})_2\}_4]$  core (583.28 g.mol<sup>-1</sup>), thus suggesting that the polymeric arrangement is not preserved; erratic results were obtained at higher concentrations in this non-coordinating solvent. Complex **2** is not sufficiently soluble for DOSY analysis in aromatic hydrocarbons.

- 16 R. Fleischer and D. Stalke, *Organometallics*, 1998, **17**, 832.
- 17 J. Eppinger, E. Herdtweck and R. Anwender, *Polyhedron*, 1998, **17**, 1201.
- 18 S. Harder, S. Mueller and E. Hübner, *Organometallics*, 2004, **23**, 178.

Accepted manuscript